MUSIC Spectra Using Cayley Graphs of Multiple-Valued Signals

Aviraj Sinha, Darrell Young, Eric C. Larson, and Mitchell A. Thornton
Darwin Deason Institute of Cybersecurity
Southern Methodist University, Dallas, TX 75205, USA
Email: {avirajs, dlyoung, eclarson, mitch}@smu.edu

***Abstract*—In this work, we propose an alternative method for generating the MUSIC (Multiple Signal Classification) pseudospectra by utilizing the spectral properties of Cayley graphs. Sensor readings are represented as multi-valued functions, which are used to color the edges connecting nodes representing symmetry permutation group elements. This graph representation yields decorrelating spectral information, enabling the effective separation of the signal subspace from the noise subspace required by the MUSIC algorithm. The proposed method is applied to a direction-of-arrival estimation task, demonstrating its ability to generate MUSIC pseudospectra for signal processing applications.**

***Index Terms*—Graph signal processing, KL transform, graph spectra, discrete function**

I. Introduction

MUSIC, first introduced in [1], is a foundational algorithm widely adopted in signal processing applications. Over the years, it has been extensively analyzed and refined [2], [3]. Its versatility has enabled its use in diverse areas such as frequency detection, direction of arrival (DOA), source localization, and acoustic and medical imaging [4]–[7]. MUSIC operates by analyzing measurements obtained from multiple sensors, which inherently correlate since they measure the same signals. The algorithm leverages the correlation between the signal space and the sensors while recognizing that the additive noise values are uncorrelated. A crucial step in the MUSIC algorithm is constructing the covariance matrix, defined as $\mathbf{R_x} = \mathrm{Cov}\{\mathbf{x}\} = \mathbb{E}\{\mathbf{x}\mathbf{x}^H\}$. This covariance matrix reveals the orthogonality between the signal and noise subspaces, as the two are uncorrelated. The eigenstructure of the covariance matrix reflects this orthogonality: the eigenvectors associated with the largest eigenvalues span the signal subspace, while those corresponding to smaller eigenvalues define the noise subspace. Consequently, the number of large eigenvalues corresponds to the number of signals. Although noise increases the rank of the covariance matrix, it is isotropic and spreads evenly, resulting in a uniform, smaller variance in all directions. This isotropy ensures that the covariance spectra typically consist of a few high values representing the signal subspace and many smaller values associated with the noise subspace.

The covariance spectra are also known as the Karhunen-Loève (KL) spectra. The KL transform has been a cornerstone technique in signal processing introduced in [8]. The KL transform has been used in many applications, including signal decorrelation and noise reduction [9]–[11]. The KL transform matrix, which is constructed from the eigenvectors of the covariance matrix, has important properties that are directly used in the MUSIC algorithm since the eigenvectors associated with the smaller eigenvalues make up the $\mathbf{U}_n$ noise subspace used in the MUSIC algorithm. This noise subspace is orthogonal to the signal subspace $\mathbf{U}_n$, as shown here: $\mathbf{U}_n\mathbf{U}_s^T = 0$. The spectral information of the standard covariance matrix is commonly used; however, in some applications, such as MUSIC, issues are associated with decorrelating signals when the number of samples is low. To address these challenges, more sample-efficient methods that use alternatives to the covariance matrix are used depending on the arrangement of the sensors. For example, a circulant matrix for circular sensor arrays or a Hankel matrix for linear sensor arrays can be used to decorrelate the signal information even from single snapshots with low noise [12], [13].

In previous work, the main goal of the spectral analysis of Cayley graphs is to minimize the representation of switching functions [14]. In other related work, Cayley graphs with different generator functions are used to obtain spectra related to that of other transforms, including Walsh and Chrestenson spectra for multiple-valued functions [15]–[17]. The previous work, [18], has shown that the Cayley graph representation of a multiple-valued function where the nodes represent the elements of a symmetry group can be used to extract spectra related to that of the KL spectra. Our work applies the method described in [18] as a way of decorrelating the signal subspace from the noise subspace while using a single snapshot of measurements as the multiple-valued coloring function. Here, a “single snapshot” refers to a single set of measurements collected simultaneously from multiple sensors. Unlike approaches that require time-averaging or multiple measurements, our method operates on this single instance of data, making it computationally efficient and suitable for applications where repeated measurements are impractical or unavailable.

In this work, we leverage the spectral properties of the Cayley graph to extract signal information from sensor readings using the MUSIC algorithm. Unlike traditional methods, our approach does not require knowledge of sensor placement or ordering. Instead, we construct a Cayley graph where the edges are colored by a multi-valued function, representing possible sensor readings for different permutations. A single snapshot measurement from all sensors is interpreted as a multi-valued coloring function applied to the graph's edges. Rather than relying on multiplications or sensor array ordering, we represent sensor readings as graph nodes connected by edges that encode their permutations. Our method samples sensor measurements from a uniform linear array (ULA) with low noise and uses single snapshot data to estimate the direction of arrival (DOA) for multiple signals. We compare the spectra and MUSIC pseudospectra obtained from the Cayley graph method to those from the standard covariance matrix. Our results demonstrate that the Cayley graph representation achieves DOA estimates comparable to the standard covariance method while eliminating the need for multiplications. Furthermore, the Cayley graph spectra closely resemble covariance-based spectra, suggesting that our method can effectively approximate covariance-based spectral information. These properties make the proposed Cayley graph method a computationally efficient alternative for generating MUSIC pseudospectra in signal processing tasks.

II. Background

A. MUSIC Pseudospectrum

Obtaining MUSIC pseudospectra is an effective method for identifying the directions or frequencies of valid signals from noisy sensor measurements, as it infers signal characteristics without requiring direct measurements at every possible value bin [1]. Instead, as shown in Equation 1, the algorithm requires a smaller set of measurements, which are used to characterize the noise subspace. This noise subspace corresponds to the eigenvectors of the covariance matrix associated with the smallest $M-K$ eigenvalues, where M is the number of sensors and K is the number of signals. To estimate the pseudospectrum, a steering vector $\mathbf{a}(\theta)$ is iteratively evaluated across potential parameter values, such as directions θ or frequencies f. The steering vector interacts with the noise subspace matrix $\mathbf{U}_n$, and the response is computed using the MUSIC spectrum formula. In Equation 1, the pseudospectrum $P(\theta)$ is calculated by evaluating the reciprocal of the projection of the steering vector onto the noise subspace. When the steering vector becomes orthogonal to the noise subspace $\mathbf{U}_n$, the denominator rapidly decreases, resulting in a sharp peak in the pseudospectrum. This peak corresponds to the valid signal parameters extracted from the noisy subspace. This pseudospectrum can be used to find multiple parameters by searching for the K largest peaks where K is the expected number of correlated signals.

$$
\begin{aligned}
P(\theta) &= \frac{1}{\mathbf{a}^H(\theta)\mathbf{U}_n\mathbf{U}_n^H\mathbf{a}(\theta)} \qquad (1)\\
\mathbf{a}(\theta) &= \begin{bmatrix}1 & e^{jkd\sin(\theta)} & e^{j2kd\sin(\theta)} & \cdots & e^{j(M-1)kd\sin(\theta)}\end{bmatrix}^T
\end{aligned}
$$

The relationship between the steering vector $\mathbf{a}(\theta)$ and the orthogonality of the signal subspace $\mathbf{U}_s$ to the noise subspace $\mathbf{U}_n$ is represented in Equation 2. This equation demonstrates that the noise and signal subspaces are orthogonal, allowing the covariance matrix $\mathbf{R}_x$ to be decomposed into additive spectral components associated with the signal and noise subspaces.

$$
\mathbf{R}_x = \mathbf{U}_s\mathbf{\Lambda}_s\mathbf{U}_s^H + \mathbf{U}_n\mathbf{\Lambda}_n\mathbf{U}_n^H \qquad (2)
$$

In Equation 3, the relationship between the sensor readings $\mathbf{X}$ and the original signal data $\mathbf{S}$ is modeled by representing the responses of multiple signals at various sensor locations, along with additive noise $\mathbf{N}$ that occurs at each measurement. In this model, $\mathbf{S}$ represents the K distinct signals, which are multiplied by the steering matrix $\mathbf{A}$. The steering matrix $\mathbf{A}$ consists of column vectors $\mathbf{a}(\theta_i)$, each corresponding to a potential signal direction or parameter. It models the spatial correlation between the sensor readings and the signals. Additive noise represents uncorrelated random fluctuations affecting the measurements.

$$
\begin{aligned}
\mathbf{X} &= \mathbf{A}\mathbf{S} + \mathbf{N} \qquad (3)\\
\mathbf{A} &= [\mathbf{a}(\theta_1), \mathbf{a}(\theta_2), \ldots, \mathbf{a}(\theta_M)]\\
\mathbf{S} &= \begin{bmatrix}s_1 & s_2 & \cdots & s_M\end{bmatrix}^T
\end{aligned}
$$

In Equation 4, we demonstrate how the covariance matrix $\mathbb{E}[\mathbf{X}\mathbf{X}^H]$ enables the separation of signal components from noise. The signal components remain correlated, while the noise components, being uncorrelated and isotropic, spread uniformly with variance σ^2 in all directions. This isotropic nature of the noise results in a noise covariance matrix proportional to the identity matrix, $\sigma^2\mathbf{I}$. The signal correlation contributes to a covariance matrix $\mathbf{R}_s$, which has rank K, corresponding to the number of signals K. Consequently, the eigenvalues associated with the signal subspace dominate, as the signal subspaces and noise subspaces are separable. The additive noise's isotropic nature results in lower eigenvalues spread uniformly across the noise subspace. This structure ensures that the largest eigenvalues of the covariance matrix $\mathbf{R}$ represent the signal subspace, while the smaller eigenvalues correspond to the noise subspace.

$$
\begin{aligned}
\mathbf{R} &= \mathbb{E}[\mathbf{X}\mathbf{X}^H] = \mathbb{E}[(\mathbf{A}\mathbf{S}+\mathbf{N})(\mathbf{A}\mathbf{S}+\mathbf{N})^H] \qquad (4)\\
&= \mathbf{A}\mathbb{E}[\mathbf{S}\mathbf{S}^H]\mathbf{A}^H + \mathbb{E}[\mathbf{N}\mathbf{N}^H]\\
&= \mathbf{A}\mathbf{R}_s\mathbf{A}^H + \sigma^2\mathbf{I}\\
\text{Rank}(\mathbf{R}_s) &= K, \quad \text{where } K \text{ is the number of signals}\\
\dim(\mathbf{U}_n) &= M-K, \quad \text{where } M \text{ is the number of sensors}
\end{aligned}
$$

B. Autocorrelation Matrix

To obtain the spectral information similar to that of the KL spectra without multiplications, we first describe the autocorrelation matrix, $\mathbf{F}$, and distinguish it from the autocorrelation function [18]. The autocorrelation function $\mathbf{R_u}$ is typically obtained by multiplying $\mathbf{F}$ with the signal, $\mathbf{f}$, as $\mathbf{R_u} = \mathbf{F}\mathbf{f}$. Our approach avoids matrix multiplication operations; instead, we analyze the spectrum of $\mathbf{F}$. $\mathbf{F}$ is data-dependent and contains statistical information by capturing repetition within the signal

[18]. Our experimental section shows how $\mathbf{F}$ results in a Cayley graph by using a symmetry group operator in its formation, enabling its spectrum to be equivalent to the KL spectrum. To construct $\mathbf{F}$ for a 1D discrete signal, we first represent the 1D signal as a vector, $\mathbf{f}$. We also represent sliding the signal $\mathbf{f}$ across various positions, denoting the shifted signals as $\mathbf{f}(\mathbf{x} \ominus \mathbf{i})$, where i is the value used to slide the signal by i samples. The sliding permutations of the signal are denoted by the $\ominus$, corresponding to a group operator, to show the shifting of the signal. The shifting before multiplication with the original $\mathbf{f}$ results in a specific response component of $\mathbf{R_u}$. We can then arrange the various $\mathbf{f}(\mathbf{x} \ominus \mathbf{i})$ values for different values of i to construct an autocorrelation matrix $\mathbf{F}$ as given in Equation 5.

$$\mathbf{F}_{\ominus} = [\mathbf{f}(\mathbf{x} \ominus \mathbf{0}), \ldots, \mathbf{f}(\mathbf{x} \ominus (\mathbf{N}-1))] \tag{5}$$

C. Symmetry Group

We use the well-known symmetry group in our formulation [19]. Previous research [18] demonstrates that the Karhunen-Loève transform spectra correlate with those from the Cayley graph associated with $\mathbf{F}$ formed using a symmetry group operator. An example symmetry group is the permutation group S_n that includes all permutations of n distinct objects, where each permutation is a rearrangement of elements and the group operator, $\circ$ is composition among the group element permutations. For instance, the group $S_3 = (S, \circ)$ represents string objects $S = abc, bca, cab, bac, cba, acb$, where each element can be considered a distinct permutation of the other elements. For example, group element bca, which represents a cyclic left shift, followed by the rearrangement represented by cab, representing a cyclic right shift, is the same as first applying the identity element represented by abc. This series of shifts can be summarized using the group notation, $(bca) \circ (cab) = (abc)$.

Definition 1. *A* ***Cayley graph*** *is a graphical representation of an algebraic group. Consider group $(G, *)$ and a subset N of G. The Cayley graph representing G with respect to N is denoted $Cay(G, N)$. The vertex set of $Cay(G, N)$ is the elements of G, and the edge contains pairs of elements from G, (x, y) such that $y = x \diamond n$ for some $n \in N$. Note that the group product operation $*$ and the generator operation $\diamond$ are not necessarily the same.*

The vertex set of the Cayley graph, discussed in Definition 1 representing a permutation group comprises vertices corresponding to $s_i \in S$ and edges defined by element pairs (s_i, s_j). A generator function is used to assign edge weights/colors in a Cayley graph. The choice of generator function is crucial, as it "chooses" the particular spectrum to be extracted. By using the operator $\circ$, the Cayley graph spectrum becomes equivalent to the KL spectrum. The Cayley graph adjacency matrix $A = [e_{ij}]$ is formed using the generator function given in Equation 6. To use this generator function, we first apply the symmetry group operation $s_i \circ s_j$; then, we apply the coloring function $f(\cdot)$, which is the original discrete signal we use to assign edge weights in the Cayley color graph.

$$e_{i,j} = f\left(s_i \circ s_j\right) \tag{6}$$

The spectrum of the Cayley graph is the set of eigenvalues of its adjacency matrix, which are the roots (including their multiplicities) of the characteristic equation of the matrix. Discussions on group theory and further explorations of Cayley graphs are elaborated in [19].

III. Cayley Graph Transform

A. Cayley Graph Generation

We use $\mathbf{F}$ in Equation 5 and replace $\ominus$ with the symmetric permutation group operator $\circ$. This notation is used since the shift permutations of the autocorrelation are a subset of the symmetric permutation operations. The resulting matrix is in Equation 7, where the j in $i \circ j$ represents a valid one-dimensional permutation of the indices before using the signal function $\mathbf{f}(\cdot)$ as each column. The operator replacement demonstrates that $\mathbf{F}$ can be described using symmetric permutation group operations by having the left side of the $\circ$ operator represent the signal index elements i, and the right side represents the symmetric permutation group element. We can further represent the signal index elements by i and thus the application of the permutation as $i \circ j$. In this notation, i can represent unique index elements across the signal, and j can represent the unique permutations.

$$\mathbf{F}_{\circ} = [\mathbf{f}(i \circ 0), \mathbf{f}(i \circ 1), \ldots, \mathbf{f}(i \circ (N-1))] \tag{7}$$

We have shown that $\mathbf{F}$ is created by applying a symmetric group operator implemented as shifting permutations on the original signal indices, enabling it to be represented as a Cayley graph. We use the generator function in Equation 6 to construct the Cayley graph using the symmetry permutation operator $\circ$ between every index element and valid permutation group element. In this Cayley graph, we can then interpret i as the starting node and j as the ending node for a directed edge. In this notation, (i, j), i is a node representing the signal index element s_i, and j is the node representing a valid permutation element s_j. Edges that connect signal indices to different permutations follow the notation $i \circ j$ since we permute the original signal index element i depending on the permutation element j. To create the graph, we simply connect every node representing a signal index element to every node representing a permutation element as an edge (i, j) with edge colors determined by the generator function in Equation 6. The function $f(\cdot)$ is defined as the original 1D signal $\mathbf{f}(\cdot)$.

Note that the indexable form of the generator Equation 6 is $e_{i,j} = \mathbf{f}^j(i)$. In this alternative function notation, $\mathbf{f}^j(i)$ is used to index the j permuted signal $\mathbf{f}$; this can also be interpreted as a function to access the precomputed i-th row and j-th column of the $\mathbf{F}$ autocorrelation. As discussed in Section II-C, edges with either the original or permuted signal values being zero would result in the edge not being present. We can keep nonzero edges as described by $E = \{(i, j) \mid \mathbf{f}^j(i) > 0\}$, $i, j \in$

V, where the permuted signal function $\mathbf{f}^j(i)$ indexed by i is used to remove edges with zero values.

The directed Cayley graph adjacency can be generated using three types of lists: source nodes, which represent signal index elements; target nodes, which represent permutation elements; and edge colors, derived from the permuted function, as demonstrated in Algorithm 1.

Algorithm 1 Generating Cayley graph

```
for j = 1 to Nrows do
    f = F[:, j]                          ▷ Select permuted function
    for i = 1 to length(f) do
        if f[i] > 0 then
            s_i ← append(s_i, i)         ▷ Index node
            s_j ← append(s_j, j)         ▷ Permutation node
            e ← append(e, f[i])          ▷ Colored using function
        end if
    end for
end for
```

B. CG for Music Pseudospectrum

Cayley graphs with symmetry group elements provide an alternative approach to approximating spectral information, similar to KL spectra, and enable applications such as the decorrelation of signal information from noisy sensor readings needed to generate the MUSIC pseudospectrum. This ability stems from the symmetric adjacency matrix of the Cayley graph, which facilitates decorrelation by leveraging its mathematical properties. Symmetric matrices, as established by the spectral theorem, have orthogonal eigenfunctions or basis vectors, enabling effective separation of signal components. For instance, the KL transform achieves maximal decorrelation by utilizing the eigenvectors of the symmetric covariance matrix to align with specific axes. Similarly, our experimental results demonstrate that the spectra of Cayley graphs, where edges are colored by sampled sensor readings, maximize zero values, mirroring the behavior of KL spectra. This highlights the Cayley graph's capability to decorrelate signals and distinguish correlated signal data from noise. The prevalence of symmetric matrices in Cayley graphs, particularly those of Abelian groups, is fundamental to achieving this decorrelation.

In Equation 8, we illustrate how the Cayley graph transforms sensor measurements $\mathbf{X}$ into decorrelated signal information by applying it to the signal-noise model previously described in Equation 3. By representing correlated signal responses as a symmetric adjacency matrix, the Cayley graph enables the decomposition of sensor readings into two components: the correlated signal, represented by $\mathbf{A}\mathbf{\Lambda}_{CG}\mathbf{A}^T$, and the isotropic noise, represented by $\sigma^2\mathbf{I}$, as shown in Equation 8. A key property of this decomposition is that the dense graph capturing noise remains isotropic, while the spectral information of the correlated signals retains a rank approximately equal to the number of signals. This separation highlights the Cayley graph's ability to effectively decorrelate sensor data.

$$\begin{aligned} CG(\mathbf{X}) &= CG(\mathbf{AS}+\mathbf{N}) \\ &= CG(\mathbf{AS}) + CG(\mathbf{N}) \\ &= \mathbf{A}\mathbf{\Lambda}_{CG}\mathbf{A}^T + \sigma^2\mathbf{I} \end{aligned} \tag{8}$$

Although the Cayley graph spectra are not identical to the KL spectra, they offer an alternative way to represent decorrelation information. Instead of calculating variance, our method evaluates the effects of multiple permutations on measured sensor values. From the Cayley graph spectra, we can analyze the degree to which the set of permutations varies the sensor measurements. For example, if a specific index node is connected to multiple permutation nodes with edges of the same value, this indicates that permutations do not impact the variation at that component and, as a result, indicate low variation. Since the connections from the index node to its permutations are all similar in value, the clustering of similar edges would result in zero values in the spectra of the adjacency matrix, a property commonly seen in spectral clustering [20].

Different function mappings may reduce the impact of permutations, grouping similar sensor readings into clusters. This grouping reduces the number of spectral coefficients required for representation. Randomly connected edges, in contrast, spread decorrelation coefficients, leading to less effective decorrelation regardless of the permutations applied. Applying a permutation matrix $\mathbf{P}$ to the original function $\mathbf{f}$ as $\mathbf{f}' = \mathbf{P}\mathbf{f}$ can further optimize the separation of the signal and noise subspaces. This optimization can be expressed as $\arg\max_{\mathbf{P}} \frac{\mathrm{Tr}(\mathbf{\Lambda}_{CG})}{\sigma^2}$. The effect of different function mappings on the spectra of Cayley graphs has been explored in [21]. Imperfect decorrelation, where some signal information mixes with the noise subspace, may require adjustments to the noise subspace, such as reducing it below the standard $M - K$ values. Nevertheless, the noise subspace is clearly represented in the eigenvectors of the Cayley graph. This illustrates the robustness of our method in extracting decorrelation information and its potential for applications where covariance-based methods are limited.

IV. Experimental Results

For our experimental results, we evaluate our method's ability to detect the directions of arrival (DoA) of multiple signals using a single snapshot. In our Cayley graph method, the single snapshot is represented as a multiple-valued coloring function $f(\cdot)$, where $f(m)$ corresponds to the m-th component of the snapshot, $x_m = a_m e^{j(m-\frac{N+1}{2})\phi_m}$. Here, a_m is the complex amplitude of the m-th plane wave, and ϕ_m is its electrical phase angle. For comparison, we construct the covariance matrix by computing the outer product $\mathbf{x}\mathbf{x}^H$, where $\mathbf{x}$ is the single snapshot. The noise power (P_{n}) is set to 1×10^{-5}, with noise modeled as a Gaussian distribution with zero mean and variance equal to the noise power. An SNR of 55 dB is used to model low-noise scenarios.

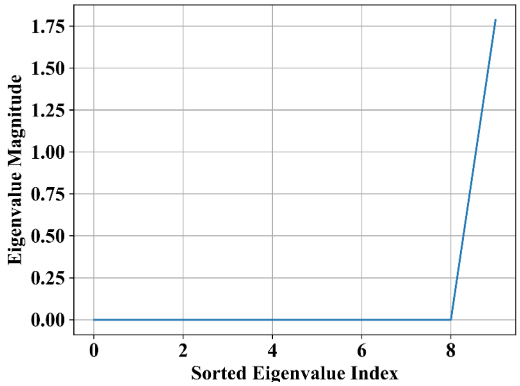

(a) Covariance-based Eigenvalues for Angles 25° and 50°

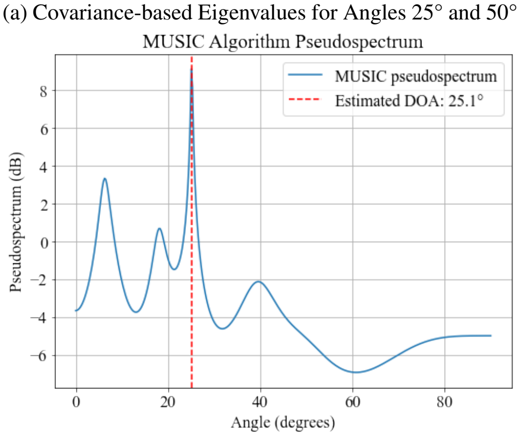

(b) Covariance-based MUSIC Spectrum for Angles 25° and 50°

Fig. 1: Covariance spectra and MUSIC pseudospectra for signals at 25° and 50° angles

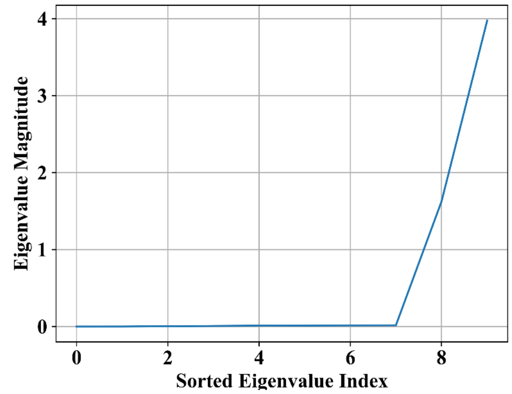

(a) CG-based Eigenvalues for Angles 25° and 50°

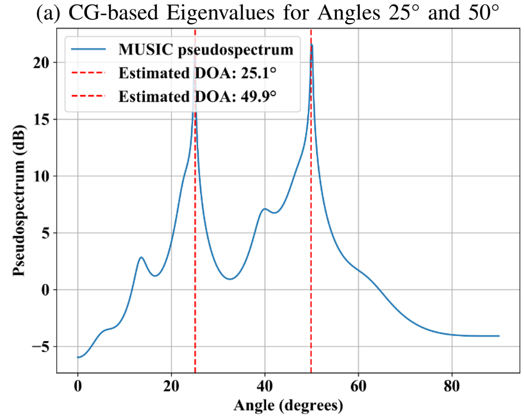

(b) CG-based MUSIC Spectrum for Angles 25° and 50°

Fig. 2: Cayley graph spectra and MUSIC pseudospectra for signals at 25° and 50° angles

For the qualitative visual results, we simulate two signals received by 10 sensors from angles of 25° and 50°. In Figure 1a, the covariance method produces only one nonzero eigenvalue, as the rank of the outer product operation is limited to one since only a single snapshot is used. From the MUSIC pseudospectrum, shown in Figure 1b, we can see the covariance method misclassifies the angles. The the largest peak us located near 25° while not detecting the second peak. This example highlights a limitation of the covariance method in the single snapshot case. While it is effective for signal decorrelation, it struggles to capture noise information from a single snapshot due to the rank deficiency of the covariance matrix. Additionally, we observe the presence of other spurious peaks, further demonstrating the challenges in accurately identifying the signal angles with this method.

The spectrum obtained using our Cayley graph transform, derived from the spectrum of the Cayley graph adjacency matrix with edges colored by the snapshot function, is shown in Figure 2a. While the number of nonzero eigenvalues is higher, the results still demonstrate a significant degree of signal decorrelation, as indicated by the presence of numerous zeros in the spectrum. However, the increased signal presence in the noise subspace is evident, with three nonzero eigenvalues observed. Despite this, our method proves to be more accurate, as shown in Figure 2b. The two largest distinct peaks in the spectrum are observed at 25.1° and 49.9°, which are very close to the expected angles of 25° and 50°. This highlights the effectiveness of our approach in accurately detecting the desired angles.

Table I provides a detailed comparison of the covariance method and the CG method for locating a single angle of arrival for 50 trials across different numbers of array elements: 10, 20, and 40. The table highlights two metrics: the mean bias, which measures the absolute error, and the standard deviation of the detected angles. The experiments were conducted with a fixed noise power of 0.1 and an angle of 45 degrees. For an array size of 10 elements, the covariance method achieves a mean bias of 0.19, which is lower than the 0.31 observed with the CG method. However, the CG method demonstrates better consistency, as indicated by its smaller standard deviation of 0.0416 compared to 0.068 for the covariance method. This suggests that while the CG method is slightly less accurate in smaller arrays, its angle estimates are more stable under noise. When the number of elements increases to 20, the CG method shows a significant improvement in accuracy, reducing its mean bias to 0.14. The covariance method maintains a lower bias at 0.06, but the CG method continues to exhibit greater stability with a standard deviation of 0.0281 compared to 0.038 for the covariance method. At 40 elements, both methods achieve similar levels of accuracy, with the mean bias being 0.06 for the covariance method and 0.07 for the CG method. The standard deviation for both methods is also very low, at 0.020 and 0.0213, respectively, indicating highly consistent angle detection results for larger arrays. These results show that while the covariance method initially has a lower bias, the CG method achieves comparable accuracy as the array size increases and consistently provides more stable estimates. This makes the CG method particularly valuable for applications that require reliable angle detection with minimal variation, especially in scenarios with larger sensor arrays.

TABLE I: Bias and variance comparison of Covariance and CG methods for angle detection. Results are averaged over 50 trials, with a test angle of 45 degrees and a constant noise power of 0.1. The table shows the mean bias and standard deviation of the detected angle for different numbers of array elements.

Number of Array Elements	**Covariance Mean Bias**	**Covariance Std Angle**	**CG Mean Bias**	**CG Std Angle**
10	0.19	0.068	0.31	0.0416
20	0.06	0.038	0.14	0.0281
40	0.06	0.020	0.07	0.0213

V. Conclusion

Our research demonstrates that the resulting Cayley graph spectra closely align with the KL spectra of multiple-valued discrete functions, resulting in comparable applications in signal decorrelation. Experimentally, we show that the Cayley graph method produces spectra and MUSIC pseudospectra similar to those generated by the standard covariance matrix, particularly in direction of arrival (DOA) applications. A notable advantage of the Cayley graph approach is its computational efficiency, as it avoids the multiplication operations required to compute the covariance matrix. Additionally, our method is versatile, as it imposes no assumptions about the placement of antennas, enabling flexibility in scenarios where antenna configurations are embedded into the matrix structure. Future work could explore extending our method to more complex sensor arrangements beyond the traditional uniform linear array (ULA) and investigate how different mappings of the coloring function impact performance. Furthermore, we can evaluate the potential for reducing computational time that comes from bypassing covariance matrix calculations. Beyond DOA, our method could also be applied to broader signal-processing tasks, including feature extraction and dimensionality reduction, to highlight its potential for diverse applications.

References

[1] R. Schmidt, "Multiple emitter location and signal parameter estimation," *IEEE transactions on antennas and propagation*, vol. 34, no. 3, pp. 276–280, 1986.

[2] B. Friedlander, "A sensitivity analysis of the music algorithm," *IEEE Transactions on acoustics, speech, and signal processing*, vol. 38, no. 10, pp. 1740–1751, 1990.

[3] R. Roy and T. Kailath, "Esprit-estimation of signal parameters via rotational invariance techniques," *IEEE Transactions on acoustics, speech, and signal processing*, vol. 37, no. 7, pp. 984–995, 1989.

[4] Z. Liu, Z. Liu, and Y. Peng, "Dimension reduction of Karhunen-Loeve expansion for simulation of stochastic processes," *Journal of Sound and Vibration*, vol. 408, pp. 168–189, Nov. 2017. [Online]. Available: https://www.sciencedirect.com/science/article/pii/S0022460X17305412

[5] I. F. Jones and S. Levy, "Signal-to-noise ratio enhancement in multichannel seismic data via the karhunen-loève transform," *Geophysical Prospecting*, vol. 35, no. 1, pp. 12–32, Jan. 1987. [Online]. Available: https://onlinelibrary.wiley.com/doi/10.1111/j.1365-2478.1987.tb00800.x

[6] P. Gupta and S. Kar, "Music and improved music algorithm to estimate direction of arrival," in *2015 International Conference on Communications and Signal Processing (ICCSP)*. IEEE, 2015, pp. 0757–0761.

[7] J. C. Mosher, S. Baillet, and R. M. Leahy, "Eeg source localization and imaging using multiple signal classification approaches," *Journal of Clinical Neurophysiology*, vol. 16, no. 3, pp. 225–238, 1999.

[8] K. Karhunen, "Zur spektraltheorie stochastischer prozesse," *Ann. Acad. Sci. Fennicae, AI*, vol. 34, 1946.

[9] J. F. Al-Asad, A. Moghadamjoo, and L. Ying, "Ultrasound image de-noising through Karhunen-Loeve (K-L) transformwith overlapping segments," in *2009 IEEE International Symposium on Biomedical Imaging: From Nano to Macro*, Jun. 2009, pp. 318–321, iSSN: 1945-8452. [Online]. Available: https://ieeexplore.ieee.org/abstract/document/5193048

[10] S. Olmos, M. Millan, J. Garcia, and P. Laguna, "ECG data compression with the Karhunen-Loeve transform," in *Computers in Cardiology 1996*, Sep. 1996, pp. 253–256, iSSN: 0276-6547. [Online]. Available: https://ieeexplore.ieee.org/abstract/document/542521

[11] J. Kittler and P. C. Young, "A new approach to feature selection based on the Karhunen-Loeve expansion," *Pattern Recognition*, vol. 5, no. 4, pp. 335–352, Dec. 1973. [Online]. Available: https://www.sciencedirect.com/science/article/pii/0031320373900253

[12] W. A. Gardner, "Simplification of music and esprit by exploitation of cyclostationarity," *Proceedings of the IEEE*, vol. 76, no. 7, pp. 845–847, 1988.

[13] W. Liao and A. Fannjiang, "Music for single-snapshot spectral estimation: Stability and super-resolution," *Applied and Computational Harmonic Analysis*, vol. 40, no. 1, pp. 33–67, 2016.

[14] A. Bernasconi and B. Codenotti, "Spectral analysis of Boolean functions as a graph eigenvalue problem," *IEEE Transactions on Computers*, vol. 48, no. 3, pp. 345–351, Mar. 1999, conference Name: IEEE Transactions on Computers. [Online]. Available: https://ieeexplore.ieee.org/abstract/document/755000

[15] M. Thornton, D. Miller, and W. Townsend, "Chrestenson spectrum computation using Cayley color graphs," in *Proceedings 32nd IEEE International Symposium on Multiple-Valued Logic*, May 2002, pp. 123–128.

[16] W. Townsend and M. Thornton, "Walsh spectrum computations using cayley graphs," in *Proceedings of the 44th IEEE 2001 Midwest Symposium on Circuits and Systems. MWSCAS 2001 (Cat. No. 01CH37257)*, vol. 1. IEEE, 2001, pp. 110–113.

[17] M. Thornton, "Mixed-radix mvl function spectral and decision diagram representation," *Automation and Remote Control*, vol. 65, pp. 1007–1017, 2004.

[18] ——, "The Karhunen-Loéve Transform of Discrete MVL Functions," in *35th International Symposium on Multiple-Valued Logic (ISMVL'05)*. Calgary, Canada: IEEE, 2005, pp. 194–199. [Online]. Available: http://ieeexplore.ieee.org/document/1423181/

[19] J. Gallian, *Contemporary abstract algebra*. Chapman and Hall/CRC, 2021.

[20] A. Ng, M. Jordan, and Y. Weiss, "On spectral clustering: Analysis and an algorithm," *Advances in neural information processing systems*, vol. 14, 2001.

[21] L. Li and M. A. Thornton, "Discrete Function KL Spectrum Computation over Symmetry Groups of Arbitrary Size," in *Proceedings of the International Symposium on Representations and Methodology of Future Computing Technologies (formerly, Reed-Muller Workshop, RMW05)*, September 2005, pp. 110–113, (with Lun Li).